DEVELOPMENT OF FORENSIC METHODS FOR THE COMPARISON OF METAL 3D PRINTING ILLICIT AND COUNTERFEIT GOODS.

By

Phillip Day

A thesis submitted in fulfilment of the requirements for the degree of

Master of Forensic Science (Professional Practice and Research)

in

The School of Medical, Molecular and Forensic Science, School of Veterinary and Life Sciences, Murdoch University

Principle Supervisor: Associate Professor James Speers

Academic Supervisors: David Parlevliet

Kari Pitts

Associate Professor Robert Mead

David Berryman

Semester 1, 2020

MURDOCH UNIVERSITY

PERTH, WESTERN AUSTRALIA

Declaration

I declare that this thesis does not contain any material submitted previously for the award of any other degree or diploma at any university or other tertiary institution. Furthermore, to the best of my knowledge, it does not contain any material previously published or written by another individual, except where due reference has been made in the text. Finally, I declare that all reported experimentations performed in this research were carried out by myself, except that any contribution by others, with whom I have worked is explicitly acknowledged.

Signed: Phillip Day

Acknowledgements

I want to thank Associate Professor James Speers, David Parlevliet at Murdoch University Engineering and Energy department, and Kari Pitts at ChemCentre, Western Australia, for their support, guidance, mentorship, and constructive feedback offered throughout this process.

Additionally, I would also like to thank Sarah Cole from Amiga Engineering Pty Ltd. and David Veale from BeSpoke 3D for their support in supplying the samples central to the study conducted.

Lastly, I would like to thank my family and friends for their constant support, guidance, patience, and encouragement. Your contributions throughout this process have been invaluable.

This work has been supported by funding from the Discipline of Medical, Molecular and Forensic Sciences, Murdoch University.

Table of Contents

Part One

Part Two

THIS PAGE HAS BEEN INTENTIONALY LEFT BLANK

Part One

Literature Review

The assessment of metal 3D printing processes for the development of forensic comparison techniques

Abstract

Three-dimensional (3D) printing is the manufacturing of objects in a layer-by-layer technique, utilising Computer-Aided Design (CAD) software and a variety of engineering processes and materials. The recent advancements and increases in the application of 3D printing have been substantially attributed to the expiry of earlier patents, resulting in new devices and processes. Criminals and organised crime groups are continually seeking new methods for the illicit manufacturing of firearms, their components and counterfeit goods, and the recent advancements and cost reductions in 3D printing technology has provided them with the means. To date, there are no published forensic studies on the assessment of the engineering features of metal 3D printing, or the application and development of forensic techniques to compare and identify the source printer and generated materials in criminal investigations. This review seeks to address this by evaluating the manufacturing and engineering features of powder bed fusion-based 3D metal printing and generated materials, and how this might assist the forensic community to apply and develop chemical and physical methods of forensic analysis.

Keywords: Forensic analysis, 3D printers, 3D printer engineering features, illicit manufacture, counterfeit goods

Table of Contents

List of Figures

List of Tables

List of Abbreviations

3D	Three-dimensional
CAD	Computer-Aided Design
DMLS	Direct Metal Laser Sintering
AFP	Australian Federal Police
OMCG	Outlaw Motorcycle Gangs
PBF	Powder Bed Fusion
SLM	Selective Laser Melting

EBM	Electron Beam Melting
Nd:YAG	Nodymium-Doped Yttrium Aluminium Garnet
Yb-Fibre	Ytterbium-Doped Optical Fibre
SEM	Scanning Electron Microscopy
EDS	Energy-Dispersive X-ray Spectroscopy
XRD	X-ray Diffraction
XRF	X-ray Fluorescence

1. Introduction

Three-dimensional (3D) printing involves the manufacturing of objects in an additive layer-by-layer technique utilising Computer-Aided Design (CAD) software and a variety of engineering processes and materials [1]. 3D printing is different from conventional manufacturing, which is a subtractive process accomplished through the removal of material from a starting object [2]. In recent years 3D printing technology has undergone significant advancement leading to novel applications using an extended range of materials, and, unlike conventional manufacturing, is not limited by the capabilities of the tools used [3]. The recent advancements have been substantially attributed to the expiry of earlier patents, resulting in new devices and processes [3]. Applications for 3D printing can be found in the automobile and medical industries, and in the aerospace Industry [4].

3D printing has been used by criminals and criminal organisations in the manufacturing of firearms and counterfeit goods [5, 6]. This came to the attention of the media in 2013, when Defense Distributed announced the 'first 3D printed' fully functional polymer firearm [7]. Further, in 2013, a 3D printed full metal firearm was manufactured by Solid Concepts using the direct metal laser sintering (DMLS) process [7]. More recently, in October 2019, homemade 3D printed firearms were used in a neo-Nazi attack on a synagogue in Germany [8]. Pavlovich [9] noted that in 2019, the Australia Border Force and Australian Federal Police (AFP) recorded an increase in attempts to illegally import polymer80 (also referred to as ghost guns) firearm components, connected with Outlaw Motorcycle Gangs (OMCG). Furthermore, as illicit firearms and firearm components are manufactured from a design file that can be obtained from the internet, or self-produced using CAD software, there are no serial numbers attached to firearms or firearm components manufactured via metal 3D printing, rendering them untraceable with current identification techniques [7]

The scale of the threat of 3D printing in the manufacture of illicit and counterfeit goods was further highlighted in a 2015 Australian parliamentary report [10], in which the Victims of Crimes Assistance League argued that the use of 3D printing by criminal groups was already being explored. The Australian Federal Police, in the same report, further noted that advancements in 3D printing technology would allow for the production of illicit and counterfeit objects [10].

However, illegal activities associated with 3D printing are not limited to the production of firearms. Hornick [11] reported that 3D printing technology was already being used to produce bank ATM skimmers, handcuff keys and drugs. He also indicated that a potential existed to generate counterfeit money. The manufacturing of military-style weapons such as IED's and other explosive devices could easily be achieved, as shown in

Table 1 [12]. Given that powder bed fusion (PBF) - based metal 3D printing is the most accessible technology, this review aims to evaluate the PBF-based 3D metal printing process and materials generated to support the application and development of forensic analytical protocols.

Table 1. Threat risk from high to low of 3D printing being used in the manufacturing of illicit and counterfeit goods [6]. Adapted from Deloitte Insights.

Threat Risk	Homemade firearms	Counterfeits	IDEs	Advanced tech/weapons
State terror		Counterfeits could enable misattribution.	Can easily make a variety of disguised devices.	Possible to build advanced devices that enable misattribution.
Non-state terror		Counterfeits could enable misattribution.	Can easily make a variety of disguised devices.	Allows small groups to create more advanced weapons that would have required a larger group of co-conspirators.
Criminal organisations	Ability to build untraceable small firearms.	Can produce counterfeit goods with only a small organised group.		
Individuals	Ability to build untraceable small firearms.	counterfeits could enable misattribution.		

2. Discussion

Metal 3D printing has undergone significant development in recent years and now has the potential to replace many conventional manufacturing practices[13]. Advancements in the types of metal powder used as starting materials, printer reliability, and the ease of sharing design files, has facilitated the development of a unique processing method for the possible manufacture of illicit and counterfeit goods. Metal 3D printing employs several different processes depending on the material and energy source used [14]. These processes and the applicability of forensic analytical techniques to distinguish between them will be discussed.

2.1. Metal 3D printing process

Powder bed fusion is one of the fastest-growing of the 3D printing technologies [15], and is defined by the International Society for Testing and Materials standards 52900 – 15 [16] as a process that selectively fuses regions of a metallic powder using thermal energy. The main 'thermal energy' processes employed are selective laser melting (SLM), direct metal laser sintering, and electron beam melting (EBM) [17]. Powder bed fusion printers are priced from as little as $6000 to more than $100,000 [18], a range that enables organised crime groups with either meagre or substantial resources to access them for illicit purposes.

The PBF printing processes are undertaken either in a partial vacuum or in the presence of an inert atmosphere, such as argon or nitrogen gas with a low oxygen content at or close to atmospheric pressure [17, 19, 20]. All PBF processes apply thin layers of powder from a reservoir to the build platform, using a roller or blade mechanism and are fused in the orientation defined by the CAD file.

2.1.1 Selective laser melting

Selective laser melting was developed with the capacity to manufacture fully dense objects (99.9 to 100% of theoretical density) that have improved mechanical properties, structural strength, stiffness and lighter weight compared to objects manufactured by conventional methods [21, 22]. The process involves depositing thin layers of very fine metallic powder, typically 20 – 100 µm in thickness [17], on a build platform. The powder in each layer are fused with a laser beam. New layers of the metallic powder are then rolled on top of previous layers and fused until the final 3D object is built [3] (Figure 1). The interaction of the laser source and the metallic powder in the bonding process generates a high-temperature gradient through heating and rapid cooling [21]. The SLM process allows for the production of objects with complex geometries through the use of support structures or scaffolding [3].

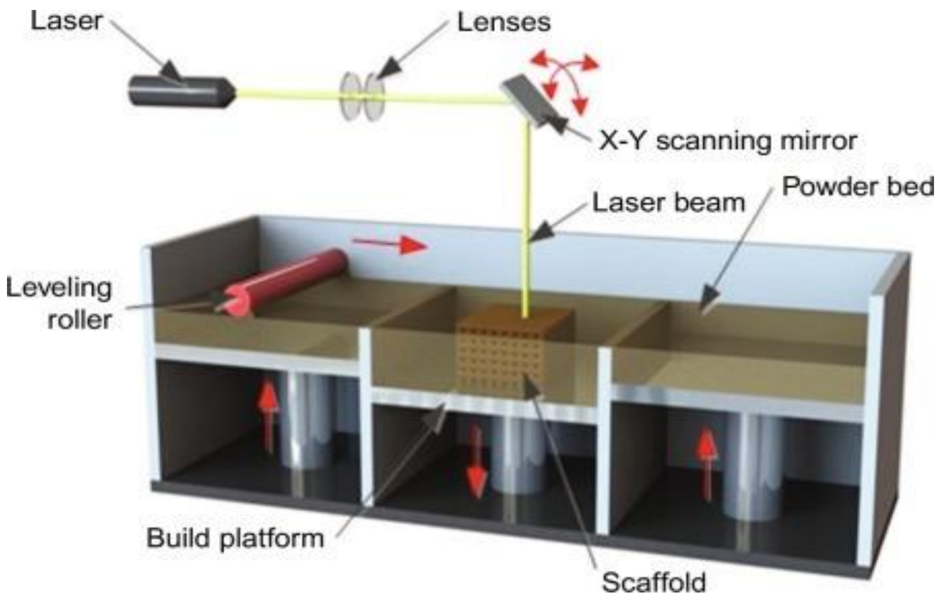

Figure 1. SLM process [23]

2.1.2 Direct metal laser sintering

Direct metal laser sintering is another laser-based PBF process used to manufacture complex parts directly from CAD models [24]. The DMLS process is similar to SLM, except solid objects are created by depositing layers of metal particles (each 20 to 60 µm in thickness) along an x/y axis using a laser beam, and selectively fusing them without completely melting the metal powder [25].

2.1.3 Electron beam melting

Electron beam melting is similar to both SLM and DMLS, except the process uses an electron beam in a vacuum chamber to melt the metal particles and fuse each layer [26] (Figure 2). Electron beam melting uses a layer of metal powder, 50 - 100 µm in thickness, heated to an optimum temperature to reduce residual stresses, and to improve mechanical properties [27]. Debroy et al. describes it as a two-step process; firstly, the prevention of electrostatic charging and particle repulsion through light sintering (solidify without liquefaction), followed by a fusing pass of the defined build volume [28].

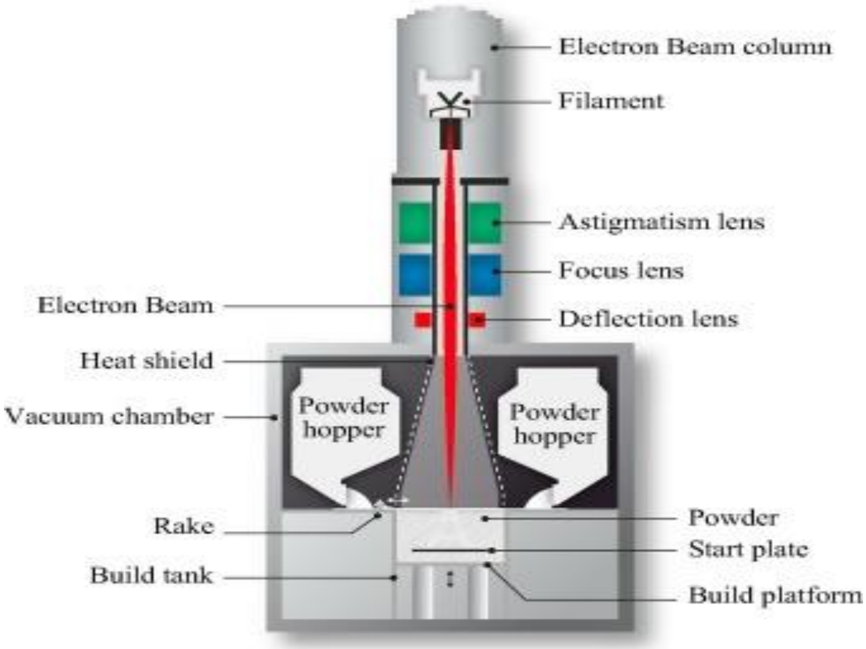

Figure 2. Schematic of the EBM process.[29]

2.2. Energy source

Crucial to a forensic investigation of metal 3D printers, is understanding how the energy source interacts with the build environment and the metal powder starting material, through laser energy intensity, heat transfer, and processing temperature. The energy source and starting material interactions, together with the resultant microstructures, will be discussed in the following section.

The PBF printers use a high energy source of a focused laser or an electron beam to selectively sinter a layer of powdered metal [30]. The laser energy used produces a photothermal reaction where heat is transferred to the metal material to either sinter or melt each layer [31]. The energy sources used in metal 3D printing include solid-state and fibre lasers [32]. The solid-state lasers typically used in SLM are neodymium-doped yttrium aluminium garnet (Nd:YAG) lasers, that use rod-shaped crystals that are optically pumped by a flash lamp or an 808 nm diode, producing a near-infrared wavelength of 1064nm [31]. The output power for Nd:YAG lasers ranges between 1 kW and 20 kW, depending on the operating mode used [31].

More recently, Ytterbium-Doped Optical Fibre (Yb-fibre) lasers have been introduced into metal 3D printing. Yb-fibre lasers utilise laser diodes operating at near infrared wavelengths of 950-980 nm or 1030-1070 nm, with the shorter wavelength generating a smaller more focused beam with a higher quality beam illumination pattern [31]. The EBM process utilises an electron gun with an operating power output of 60kW and a focus beam energy of greater than 100 kW/cm^2; electromagnetic lenses control the focus of the beam [26].

The wavelength, laser energy, pulse duration and the quality of the starting materials will affect the melting and solidification process of the metal[31] and potentially affect the microstructure of the finished product. This is discussed in the next section.

2.3. Metal Powders

The typical feedstock (metallic powdered materials) used in PBF-based technologies consist of stainless steel, aluminium and nickel-based alloys, and titanium and its alloys (Table 2) [3]. They are typically chosen because they are lightweight with high tensile strength, hardness, and wear resistant compared to those used in conventional manufacturing [3]. The specific process performance of the metal powders are defined by their chemical properties and physical characteristics including surface morphology, flowability, particle shape and size (typically in the range of 10 – 60 µm) [27, 32] The processing of the various metals is dependent upon their differences in laser absorption, surface tension, and viscosity [21].

Table 2. Standard metal powders used in each of the PBF processes.

Processes	Metal Powders				
	Aluminium Alloys	Stainless Steel	Nickel Alloys	Titanium Alloys	Cobalt Alloys
SLM	$AISi_{10}Mg$ $AISi_{7}Mg0.6$ $AISi_{9}Cu3$	316L	IN625 IN718 IN939	Ti6AI4V	$CoCr_{28}Mo_{6}$
DLSM	$AISi_{10}Mg$	316L 17 -4 PH	IN625 IN718	Ti6AI4V Ti64	CoCrMo
EBM				Ti6AI4V ELI Ti Grade 2	ASTM F75 CoCr alloy

The metal powders are manufactured using water, gas or plasma atomisation [30] and the different methods used in their manufacture generate differences in particle morphology, particle size, and chemical composition [33] (Figure 3). These physical and chemical characteristics of the metallic powder determine its density and flowability [30]. Several studies have reported that the morphological properties of the metallic powders can influence both the surface roughness and the density of metal 3D-printed objects [34]. Aboulkhair et al. [35] reported that metal powders showed variability in the morphological properties of the powder, and the powder chemical specifications between manufacturers morphological properties of the powder, and the powder chemical specifications between manufacturers.

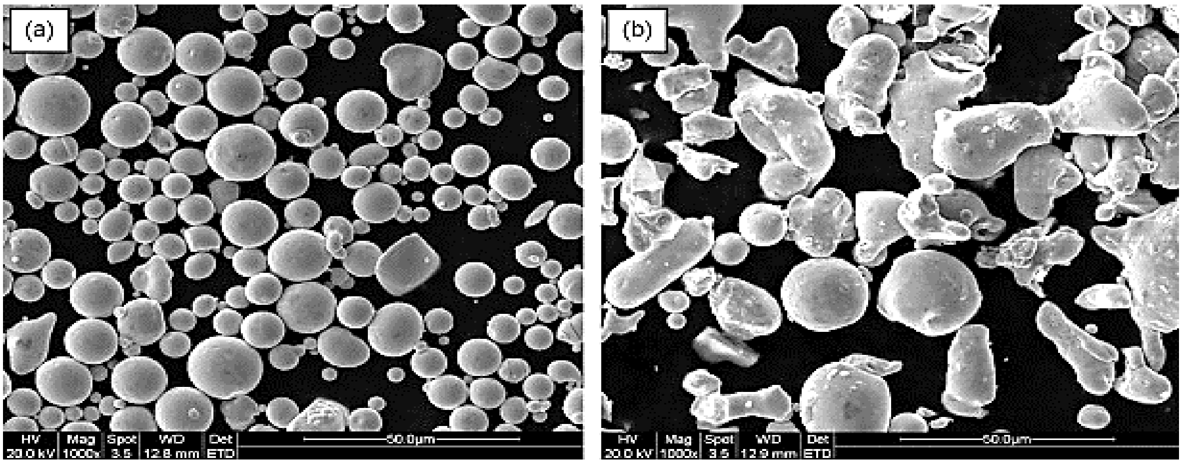

Figure 3. Powder morphology of stainless-steel powder from two different manufacturing methods. (a) gas atomisation: (b) water atomisation. [36]

Furthermore, Rafi et al.[37] found that objects manufactured with the SLM process had smoother surfaces than those manufactured using the EBM process. Metallic powders with highly reflective surfaces, such as aluminium alloys, have high thermal conductivity and a capacity to absorb fibre laser energy in the infrared wavelength region [38]. The high thermal conductivity of aluminium alloy powders reduces thermally-induced stress [33]. The surface chemistry of metallic powders subsequently affects the ability of the melted powder to flow [34]. Final objects generated from powders with coarse surface textures and irregular particle shape, display higher surface roughness [28]. The extent of surface variability between objects generated by each of the three metal 3D printing processes is shown in of approximately 1.06 µm [38]. The high thermal conductivity of aluminium alloy powders reduces thermally induced stress [33]. The surface chemistry of metallic powders subsequently affects the ability of the melted powder to flow [34]. Powders with coarse surface textures and exhibiting irregular particle shape, show higher surface roughness in the final object [28]. The extent of the surface variability between objects generated by each of the three metal 3D printing processes is shown in Figure 4.

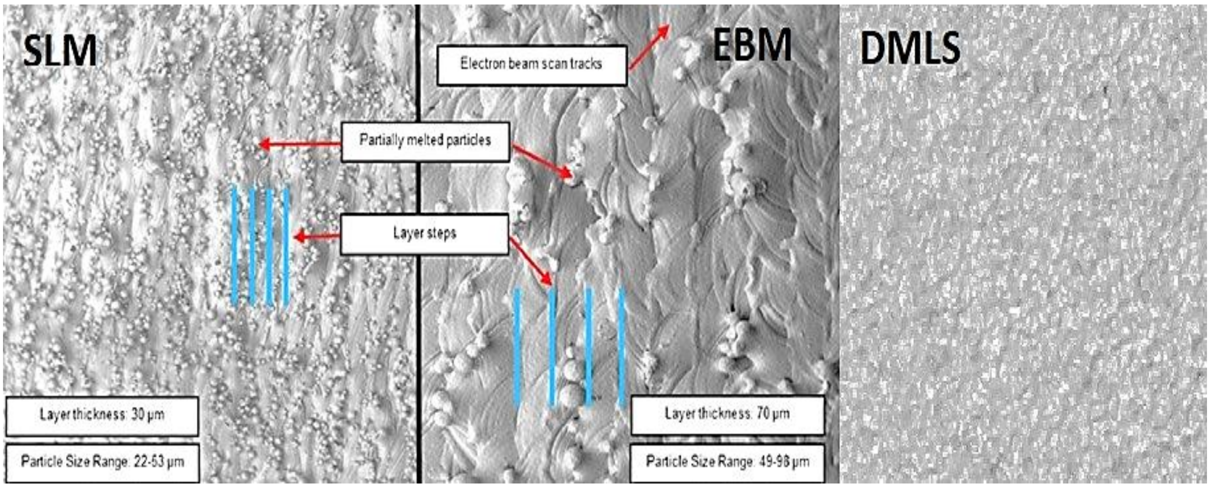

Figure 4. Differences in surface roughness between objects generated by the SLM, EBM, and DMLS processes.[39, 40]

Microstructure-variation within the metallic powder samples potentially affect the characteristics of the printed object [34]. Microstructures occur when insufficient energy is applied to highly reflective powders, resulting in partial melting and fill defects generated in the build layer [38]. In the SLM process, when aluminium powders are used, microstructures occur due to repeated melting and cooling of the build layers [21]. Lam et al. [41] found that in the SLM process, tree-like crystal microstructures together with a network of super-lattice microstructures were generated as the melted aluminium powder solidified (Figure 6). Furthermore, Rafi et al. [37] reported, that when titanium powder was used in the SLM process, martensitic microstructures formed but in the EBM process, the lamellar morphology of Widmanstatten/basketweave microstructures was evident (Figure 5).

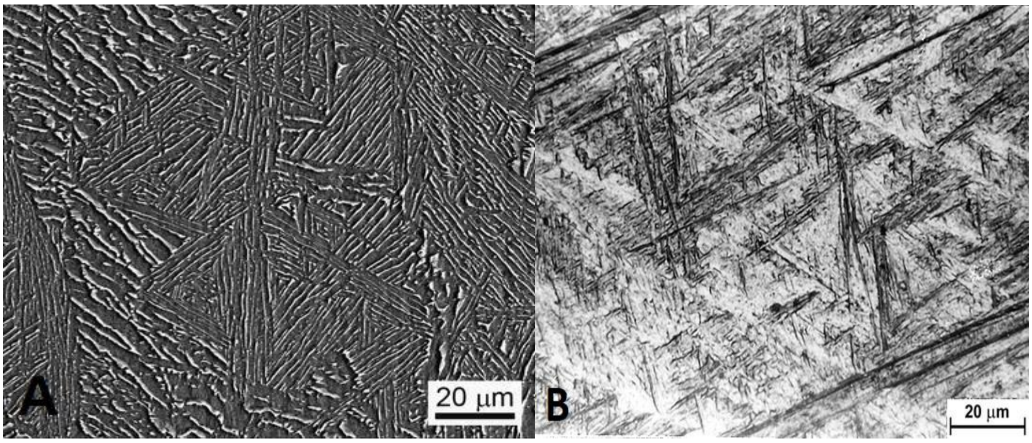

Figure 5. Titanium powder showing: A) Widmanstatten microstructure, B) Martensitic microstructure.[37, 42]

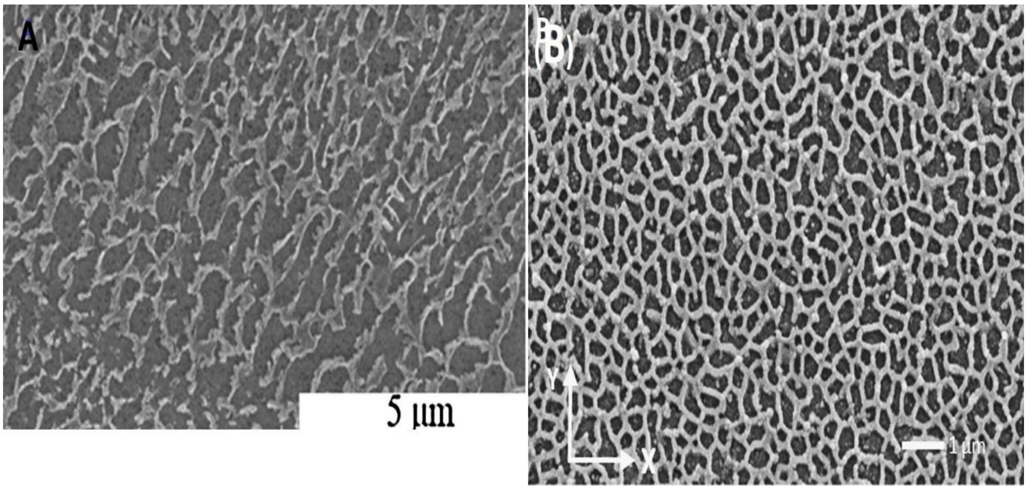

Figure 6. Differences in the tree-like microstructure formation of aluminium alloy in a) SLM, b) DMLS [43, 44]

Pore formation may also occur during the atomisation of the metal powders. This porosity can originate from the powder or as an outcome of the process. Process-induced porosity forms when the energy from the laser is inadequate to completely melt the powder, resulting in a lack of fusion of the powder layer. The pores are typically non-spherical, uniformly distributed and of varying sizes [30, 45]. Taha et al. [46] postulated that pore formation could occur between the powder particles or between the build layers while Cherry et al. [45] reported that pore formation occurred in 316L stainless steel when low laser energy density was used in the SLM process [45]. Thijs et al. [47] found pore and oxide microstructures in aluminium material used in the SLM process as seen in Figure 7. Cherry et al. [45] also found that pore formation occurs in 316L stainless steel when low laser energy density is used in the SLM process [45]. Abourlkhair at el. [35] further found that during the SLM process balling microstructures can form (Figure 8. Balling microstructures formation in aluminium alloys during the SLM process. [35]).

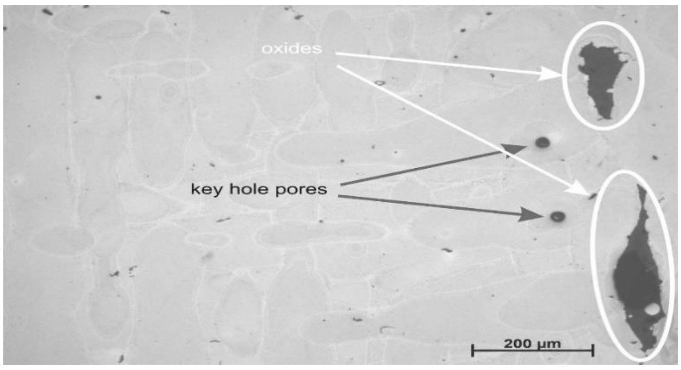

Figure 7. Pore and oxide microstructures in aluminium alloys of the SLM process. [47]

Figure 8. Balling microstructures formation in aluminium alloys during the SLM process. [35]

3. Forensic Analysis

To date, there are no published reports which forensically assess, the features generated by the different engineering protocols used in metal 3D printing that may facilitate the comparison of materials and the identification of the source printer. Because of a lack of forensic research on the properties of the powders, the interaction between the powders, the printing processes used, and the nature of the microstructures generated, there are significant knowledge gaps, that if addressed, may help to establish the provenance of illegally manufactured objects.

The part design, build strategy, and printer hardware has the potential to affect the printing parameters. The influence of the laser wavelength and temperature of the build chamber determined by the printing parameters affects the porosity of the powder causing pore formation along with part cracking and deformation. The interplay connecting the printing parameters are system defined and operator controlled potentially affecting the final object. The build chamber atmosphere being argon, nitrogen gas or a vacuum and the quality of the powder material result in the interaction between the heat transfer within the printing parameters and the powder material possibly affecting the material chemistry. The influence of the printing parameters, quality of the powder, and material chemistry further has an influence on the rate of cooling after the laser has passed over the material introducing the microstructures to the build process (Figure 9).

Due to the complexity of the interaction between the printing process, the printer hardware, and the printing materials, as shown in Figure 9**Error! Reference source not found.**, a thorough knowledge of the printing processes, the metal powders and their properties, together with the generated microstructures are crucial to the potential differentiation between metal 3D printers and the objects produced by them.

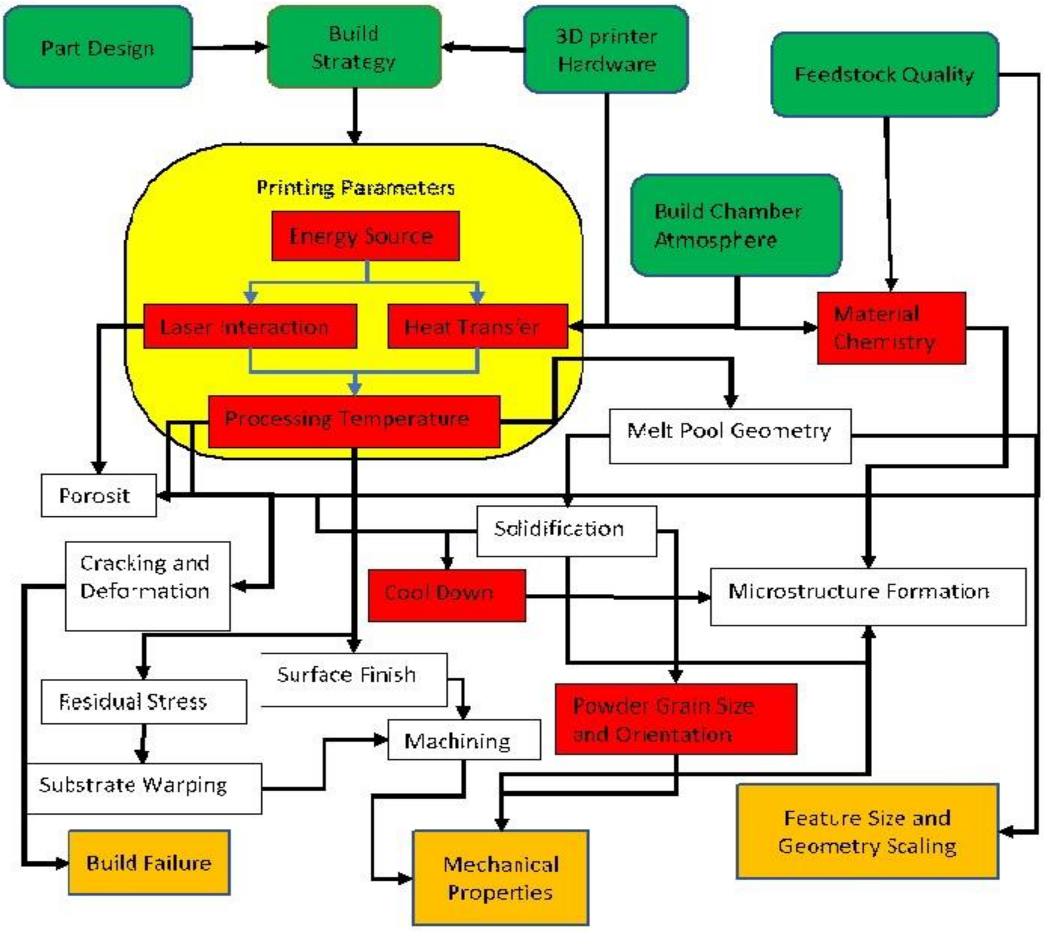

Figure 9. Process flowchart for metal 3D printing Showing how interactions between printer hardware, process, and printing materials could affect the final object. Areas in red all have the potential to influence microstructures within the final object [48] . Adapted from IEEE Global Specs.

4. Research focus

Tool mark comparison and impression analyses are standard approaches which can assist in the determination of the provenance of conventionally manufactured objects [49]. Ongoing research is directed at characterising the physical features of 3D printed metal material surfaces and their associated microstructures, using low and high-powered microscopy, scanning electron microscopy (SEM) coupled with energy-dispersive X-ray spectroscopy (EDS). In addition, the analysis of the chemical composition of 3D printed material using X-ray diffraction (XRD), and X-ray fluorescence (XRF) to determine if there are any significant differences between powders derived from different manufactures.

5. Experimental aims and hypothesis

This literature review has identified the current processes used in metal 3D printing, possible physical and chemical variations of surface morphology in the metallic powder materials, and microstructures within the build layers where it may be possible to identify the printer source of the 3D printed object.

This research aims to evaluate the potential to identify differences in metal 3D printed objects, through chemical and physical analysis of the metal printing processes and printing materials. It is proposed that any differences in metal 3D printed objects will be due to the metal printing processes. The differences in the metal printed objects are proposed to be the result of microstructures within the layers from the printing process. Accordingly, the hypothesis to be tested is:

Hypothesis 1

H_0: Physical and chemical analysis will not be able to identify differences between 3D metal printed materials.

H_1: Physical and chemical analysis will be able to identify differences between 3D metal printed materials.

6. Experimental design

Analysis of the surface structures of metal 3D printed objects assesses the homogeneity of the metal objects with attention to cracks and other imperfections of microscopic nature. In order to assess 3D metal objects for the development of forensic methods in the comparison of metal 3D printing illicit and counterfeit goods, a simple geometric object will be designed using CAD software to be manufactured using both DMLS and SLM printing processes as depicted in figure 8.

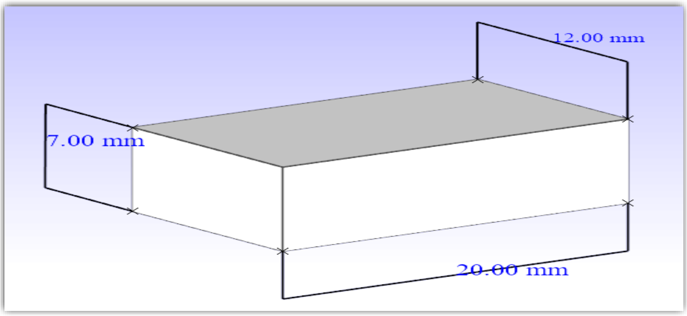

Figure 10. Computer-Aided Design of samples to be obtained from local 3D printing companies, showing the dimensions of the printed object.

Microscopy is commonly used in the 3D printing industry due to its ability to quantitatively and qualitatively measure the size, shape, and surface roughness of the metal particles [34]. The samples obtained will be analysed for any surface structures from the printing process that might be present within the layer formation. The analysis will compare the surface structure formation between the two different processes as well as within each of the DMLS and SLM process.

6.1. Scanning electron microscopy analysis

Scanning electron microscopy is an investigative tool that uses a beam of focused electrons to produce high magnification images for particle and surface characterisation [50]. The chemistry of SEM characteristics of metal material is the result of interactions with the electron beam and the metal material. The physical analysis of each metal object to identify potential printer signatures will be conducted using SEM.

6.2. Energy Dispersive X-ray Spectroscopy analysis

Energy-dispersive X-ray spectroscopy analysis is an analytical technique used in conjusction with SEM for the elemental analysis or chemical characterization of a sample. The EDS analysis can be used to determine the elemental composition of individual points or to map out the lateral distribution of elements from the imaged area.

6.3. X-ray diffraction analysis

X-ray diffraction analysis determines the crystal structures of metal materials to ascertain which crystalline phase is present in the metal material. Through the examination of diffraction peaks, XRD analysis provides a qualitative and semi-quantitative determination of crystalline structures of the metal materials [51]. Phase identification is typically achieved using the International Centre for Diffraction Data [52]. The analysis of 3D printed samples for the comparison of metal 3D printing of illicit and counterfeit goods will be conducted using XRD.

7. Conclusion

This paper has discussed three of the metal powder bed fusion-based technologies, with the aim of identifying potential areas in which metal 3D printing could be used in the commission of illicit and counterfeit goods. Particular reference has been made to the illegal manufacture manufacturing of firearms and firearm components. The This review identifies a current research gap, which if addressed, may allow metal 3D printed materials produced by different methods and/or using diverse materials to be identified. To assist in this aim, the physical and chemical features which can be used to distinguish between these variables have also been addressed. Research aimed at comparing the metal materials and processes used so as to characterise the physical and chemical variations within 3D-printed metal objects, is essential if forensic protocols are to be developed to assist in provenance determination for counterfeit and illicit goods.

8. References

1. Berman B. 3-D printing: The new industrial revolution. Business horizons. 2012;55(2):155-62.
2. Jensen-Haxel P. 3D printers, obsolete firearm supply controls, and the right to build self-defense weapons under Heller. Golden Gate UL Rev. 2011;42:447.

3. Ngo TD, Kashani A, Imbalzano G, Nguyen KTQ, Hui D. Additive manufacturing (3D printing): A review of materials, methods, applications and challenges. Composites Part B. 2018;143:172-96.
4. Campbell T, Williams C, Ivanova O, Garrett B. Could 3D printing change the world. Technologies, Potential, and Implications of Additive Manufacturing, Atlantic Council, Washington, DC. 2011.
5. Pîrjan A, Petrosanu DM. The impact of 3D printing technology on the society and economy. Journal of Information Systems & Operations Management. 2013:1.
6. Stehn M, Wing I, Carlile T, Dichairo J, J Marini. 3D opportunity for adversaries Additive manufacturing considerations for national security [internet]: Deloitte insights; 2017 [Available from: https://www2.deloitte.com/us/en/insights/focus/3d-opportunity/national-security-implications-of-additive-manufacturing.html#endnote-sup-7.
7. Jenzen-Jones N. Small arms and additive manufacturing: An assessment of 3D-printed firearms, components, and accessories. In: King B, McDonald G, editors. Behind the Curve: New Technologies, New Control Challenges. Switzerland: Small Arms Survey; 2015. p. 43.
8. German Synagogue Attacker Used Homemade 3D-Printed Plastic Gun. *Homeland Security News Wire*. 2019 10 October
9. Pavlovich S. 3D print applications of illicit firearms manufacture: A review [RMT. Thesis]. Perth, Australia: Murdoch University; 2019.
10. Legal Senate, Committee Constitutional Affairs References. Inquiry into the ability of Australian law enforcement authorities to eliminate gun-related violence in the community. Commonwealth of Australia. Extraído de; 2015.
11. Hornick J. 3D Printing New Kinds of Crime Alexandria, VA International Association of Chiefs of Police; [cited 2019 Dec 12]. Available from: https://www.policechiefmagazine.org/3d-printing-new-kinds-of-crime/?ref=05ceb1d39d8b832ee7ab768f8919f9d2.
12. Grunewald S. The FBI Wants to Use a Stratasys Objet24 to Study the 3D Printed Bombs of the Future. [internet] 2014 [cited 2019 Dec 12]. Available from: https://3dprintingindustry.com/news/3d-printed-bombs-fbi-stratasys-objet24-28438/.
13. Understanding Design & Process of DMLS 3D Metal Printing [internet] 2018 [cited 2019 Dec 11]. Available from: https://grabcad.com/tutorials/how-to-get-the-most-out-of-3d-metal-printing.
14. Duda T, Raghavan LV. 3D metal printing technology. IFAC-PapersOnLine. 2016;49(29):103-10.
15. Ashish, Ahmad Nabeel, Gopinath P., Vinogradov Alexandr. Chapter 1 - 3D Printing in Medicine: Current Challenges and Potential Applications. In: Ahmad N, Gopinath P, Dutta R, editors. 3D Printing Technology in Nanomedicine: Elsevier; 2019. p. 1-22.
16. ISO. ASTM52900-15, Standard Terminology for Additive Manufacturing – General Principles – Terminology. West Conshohocken, PA,: ASTM International; 2015.
17. Bhavar V, Kattire P, Patil V, Khot S, Gujar K, Singh R. A review on powder bed fusion technology of metal additive manufacturing. Additive Manufacturing Handbook: CRC Press; 2017. p. 251-3.
18. Cherdo L. The best metal 3D printers in 2019 2019 [updated Jul 4, 2019]. Available from: https://www.aniwaa.com/best-of/3d-printers/best-metal-3d-printer/.

19. Bidare P, Bitharas I, Ward RM, Attallah MM, Moore AJ. Laser powder bed fusion in high-pressure atmospheres. The International Journal of Advanced Manufacturing Technology. 2018;99(1-4):543-55.
20. Kalms M, Narita R, Thomy C, Vollertsen F, Bergmann RB. New approach to evaluate 3D laser printed parts in powder bed fusion-based additive manufacturing in-line within closed space. Addit Manuf. 2019;26:161-5.
21. Trevisan F, Calignano F, Lorusso M, Pakkanen J, Aversa A, Ambrosio E, et al. On the selective laser melting (SLM) of the AlSi10Mg alloy: process, microstructure, and mechanical properties. Materials. 2017;10(1):76.
22. Kruth JP, Mercelis P, Van Vaerenbergh J, Froyen L, Rombouts M. Binding mechanisms in selective laser sintering and selective laser melting. Rapid prototyping journal. 2005;11(1):26-36.
23. Vyas C, Poologasundarampillai G, Hoyland J, Bartolo P. 3D printing of biocomposites for osteochondral tissue engineering. Biomedical Composites. Second ed. University of Manchester, Manchester, United Kingdom: Woodhead Publishing Series in Biomaterials; 2017. p. 261-302.
24. Dupláková D, Hatala M, Duplák J, Radchenko S, Steranka J. Direct Metal Laser Sintering – Possibility of Application in Production Process. SAR Journal. 2018;1(4):123-7.
25. Castells R. DMLS vs SLM 3D Printing for Metal Manufacturing [internet]. Element Materials Technology; 2016 [cited 2019 Sept]. Available from: https://www.element.com/nucleus/2016/06/29/dmls-vs-slm-3d-printing-for-metal-manufacturing.
26. Sing SL, An J, Yeong WY, Wiria FE. Laser and electron-beam powder-bed additive manufacturing of metallic implants: A review on processes, materials and designs: LASER AND ELECTRON-BEAM ADDITIVE MANUFACTURING OF METALLIC IMPLANTS. Journal of Orthopaedic Research. 2016;34(3):369-85.
27. 3dsourced. Electron Beam Melting: Everything You Need To Know About EBM 3D Printing 2018 [Available from: https://3dsourced.com/3d-printing-technologies/electron-beam-melting-ebm/.
28. DebRoy T, Wei HL, Zuback JS, Mukherjee T, Elmer JW, Milewski JO, et al. Additive manufacturing of metallic components–process, structure and properties. Progress in Materials Science. 2018;92:112-224.
29. Additively. Electron Beam Melting (EBM) [internet] 2018 [cited 2019 25 Sept]. Available from: https://www.additively.com/en/learn-about/electron-beam-melting.
30. Sames WJ, List FA, Pannala S, Dehoff RR, Babu SS. The metallurgy and processing science of metal additive manufacturing. International Materials Reviews. 2016;61(5):315-60.
31. Lee H, Lim CHJ, Low MJ, Tham N, Murukeshan VM, Kim YJ. Lasers in additive manufacturing: A review. International Journal of Precision Engineering and Manufacturing-Green Technology. 2017;4(3):307-22.
32. Das S, Bourell DL, Babu SS. Metallic materials for 3D printing. MRS Bulletin. 2016;41(10):729-41.
33. Herzog D, Seyda V, Wycisk E, Emmelmann C. Additive manufacturing of metals. Acta Materialia. 2016;117:371-92.
34. Sutton AT, Kriewall CS, Leu MC, Newkirk JW. Powder characterisation techniques and effects of powder characteristics on part properties in powder-bed fusion processes. Virtual and Physical Prototyping. 2017;12(1):3-29.

35. Aboulkhair NT, Maskery I, Ashcroft I, Tuck C, Everitt NM, editors. The role of powder properties on the processability of Aluminium alloys in selective laser melting. 22nd World of Photonics Congress: Lasers in Manufacturing conference; 2015.
36. Li R, Shi Y, Wang Z, Wang L, Li J, Jiang W. Densification behavior of gas and water atomized 316L stainless steel powder during selective laser melting. Applied Surface Science. 2010;256(13):4350-6.
37. Rafi HK, Karthik NV, Gong H, Starr TL, Stucker BE. Microstructures and mechanical properties of Ti6Al4V parts fabricated by selective laser melting and electron beam melting. Journal of materials engineering and performance. 2013;22(12):3872-83.
38. Aboulkhair NT, Simonelli M, Parry L, Ashcroft I, Tuck C, Hague R. 3D printing of Aluminium alloys: Additive Manufacturing of Aluminium alloys using selective laser melting. Progress in Materials Science. 2019;106.
39. Manfredi D, Calignano F, Krishnan M, Canal R, Ambrosio EP, Biamino S, et al. Additive manufacturing of Al alloys and aluminium matrix composites (AMCs). Light metal alloys applications: IntechOpen; 2014.
40. Triantaphyllou A, Giusca C, Macaulay G, Roerig F, Hoebel M, Leach R, et al. Surface texture measurement for additive manufacturing. Surface Topography: Metrology and Properties. 2015;3:024002.
41. Lam LP, Zhang DQ, Liu ZH, Chua CK. Phase analysis and microstructure characterisation of AlSi10Mg parts produced by Selective Laser Melting. Virtual and Physical Prototyping. 2015;10(4):207-15.
42. Sieniawski J, Ziaja W, Kubiak K, Motyka M. Microstructure and mechanical properties of high strength two-phase titanium alloys. Titanium Alloys-Advances in Properties Control. 2013:69-80.
43. Wei Pei, Wei Zhengying, Chen Zhen, Du Jun, He Yuyang, Li Junfeng, et al. The AlSi10Mg samples produced by selective laser melting: single track, densification, microstructure and mechanical behavior. Applied Surface Science. 2017;408:38-50.
44. Yan Chunze, Hao Liang, Hussein Ahmed, Young Philippe, Huang Juntong, Zhu Wei. Microstructure and mechanical properties of aluminium alloy cellular lattice structures manufactured by direct metal laser sintering. Materials Science and Engineering: A. 2015;628:238-46.
45. Cherry JA, Davies HM, Mehmood S, Lavery NP, Brown SGR, Sienz J. Investigation into the effect of process parameters on microstructural and physical properties of 316L stainless steel parts by selective laser melting. The International Journal of Advanced Manufacturing Technology. 2015;76(5-8):869-79.
46. Taha MA, Yousef AF, Gany KA, Sabour HA. On selective laser melting of ultra high carbon steel: Effect of scan speed and post heat treatment. Materialwissenschaft und Werkstofftechnik. 2012;43(11):913-23.
47. Thijs Lore, Kempen Karolien, Kruth Jean-Pierre, Van Humbeeck Jan. Fine-structured aluminium products with controllable texture by selective laser melting of pre-alloyed AlSi10Mg powder. Acta Materialia. 2013;61(5):1809-19.
48. Kardys G. Factors to Consider When 3D Printing or Additive Manufacturing Metal Parts [internet]. 2017 [cited 2019 Nov 20]. Available from: https://insights.globalspec.com/article/7447/factors-to-consider-when-3d-printing-or-additive-manufacturing-metal-parts.
49. Day PJ, Speers SJ. The assessment of 3D printer technology for forensic comparative analysis. Australian Journal of Forensic Sciences. 2019:1-11.

50. Postek Michael T, Howard Karen S, Johnson Arthur H, McMichael Kathlyn L. The scanning electron microscope. Handbook of charged particle optics. 1997:363-99.
51. Slotwinski John A, Garboczi Edward J, Stutzman Paul E, Ferraris Chiara F, Watson Stephanie S, Peltz Max A. Characterization of metal powders used for additive manufacturing. Journal of research of the National Institute of Standards and Technology. 2014;119:460.
52. International Centre for Diffraction Data [Available from: http://www.icdd.com/.

THIS PAGE HAS BEEN INTENTIONALY LEFT BLANK

Part Two

Manuscript

Comparison of Powder Bed Fusion Metal 3D Printing for the Development of Forensic Methods

Abstract

Criminals and organised crime groups are continually seeking new and innovative methods, and the recent advancements in 3D printing technology, along with the reduction in the cost of 3D printers, has provided them with the means for the manufacturing of illicit goods including firearms and their components. Powder Bed Fusion is the primary 3D metal printing technology with the Direct Metal Laser Sintering or Selective Laser Sintering processes using high energy lasers to selectively sinter a layer of powdered metal. To date, there are no studies on the assessment of the engineering features of metal 3D printing, to support the development of forensic techniques to compare and identify the source printer and generated materials in aiding law enforcement in criminal investigations. This research aims to evaluate the potential to identify differences in PBF based 3D metal printers and generated materials using chemical and physical analysis, for the development of forensic methods which can be used by the forensic community.

Key Words: Forensic techniques, 3D printers, 3D printer engineering features, illicit manufacture, counterfeit goods

Table of Contents

List of Figures

List of Tables

List of Abbreviations

3D	Three-dimensional
Al	Aluminium
ASTM	American Society for Testing and Materials
CAD	Computer-Aided Design
DMLS	Direct metal laser sintering
EBM	Electron beam melting
PBF	Powder bed fusion
SEM	Scanning electron microscopy
Si	Silicon
SLM	Selective laser melting
SLS	Selective Laser Sintering
XRD	X-ray diffraction

1. Introduction

Three dimensional printing has seen applications in the medical and automobile industry, aerospace applications, and the fashion industry [1]. However there is an increased possibility of 3D printing being used in criminal activities [2]. Criminals and organised crime groups are continually seeking new and innovative methods, and the recent advancements in 3D printing technology, along with the reduction in the cost of 3D printers, has provided organised crime groups with the potential to manufacturing of illicit goods. 3D printing uses several different processes, depending on the materials used. Metal 3D printing has seen significant growth and has the potential to replace many conventional manufacturing practices [3]. Advancements in the types of metal powder starting materials, printer reliability, enhanced metal performance along with the ease of sharing design files have enabled a unique processing method for the possible manufacture of illicit and counterfeit goods. Metal 3D printing uses several different processes, depending on the material and energy source used [4]. Powder Bed Fusion (PBF) is one of the fastest-growing of the 3D printing technologies [5] and is defined by the International Society for Testing and Materials (ASTM) standards 52900 – 15, as a process that uses thermal energy to selectively fuse regions of a metallic powder [6]. The main PBF processes are Direct Metal Laser Sintering (DMLS), Selective Laser Sintering (SLM) [7]. Both SLM and DMLS processes can manufacture near dense objects, with structural strength, stiffness, that are noticeably lighter weight than those manufactured conventionally [8, 9]. These processes use high energy lasers to selectively sinter a layer of powdered metal [10]. The primary processing parameters of PBF based technologies are the high energy laser source, and the powdered metal materials [7].

Metallic materials used in PBF based technologies typically consist of aluminium alloys, stainless steel, titanium and its alloys, and nickel-based alloys [11]. The properties of the individual powders can be defined through their physical and chemical properties, the behaviour of the powder, and the specific process performance of the powder [12]. These properties include the particle shape, size, surface morphology, and flowability of the metallic powders, with typical particle sizes in the range of 10 – 60 µm [13]. These metallic materials are typically lightweight, with high tensile strength, hardness, and wear resistance compared to conventional manufacturing [11].

Forensic techniques have yet to be applied to the analysis and comparison of different metal 3D printers', through the identification of engineering features and printing material composition for the identification of intrinsic (variations of printer hardware imperfections) and extrinsic (variations added in the print process) signatures passed on to the printed object [2]. The forensic examination of physical evidence is used in the discriminating comparison of collected crime scene evidence with reference material, as well as the classification of evidence samples according to their specific chemical and physical properties [14]. One powerful tool used in forensic analysis is scanning electron microscopy (SEM) and when equipped with energy dispersive X-ray spectrometry (EDX) it can examine evidentiary material through simultaneously examining the morphology and the elemental composition of object [14]. X-ray diffraction (XRD) is another tool used widely in forensic science in the analysis and comparison of crystalline materials from heavy metals to organic compounds [15]. For metals and alloy analysis, XRD can also be used to determine the phase of the metal material [15].

To date, there are no studies on the assessment of the engineering features of metal 3D printing to support the development of forensic techniques to compare and identify the source printer and materials generated. It is proposed that any differences in metal 3D printed object will be due to the chemical and physical properties of 3D printing metal processes. This research aims to evaluate this through the following objectives.

- To assess the engineering features of metal 3D printing, to support the development of forensic techniques to compare materials and identify the source printer.
- To identify suitable techniques that can be used by the forensic community.

2. Materials and Methods

Fourteen aluminium alloy (AlSi10Mg) samples measuring 20 X 12 X 7 mm were produced using SLM and DLMS processes. Ten of the samples were fabricated as built without any surface finishing and four finished by machining and polishing to supplier's specification. (Figure 1). Additionally, approximately 50mL of the raw AlSi10Mg powder was also obtained from both suppliers for characterisation.

The system used to produce the SLM samples was an SLM 280 HL equipped with 400W fibre laser, with a wavelength of 1070nm in an argon inert gas atmosphere. The aluminium powder used to produce the seven SLM samples has the chemical composition shown in Table 1, and particle size was 20-63µm and spherical shape as provided by the manufacture. The SLM samples were produced at 30µm layer resolution with an average surface roughness of 5-5.5 Ra [µm]. The seven DMLS samples manufactured on a ProX320 system equipped with a 500W fibre laser at a wavelength of 1070nm in an argon gas atmosphere. The aluminium powder used in the ProX320 has the chemical composition as provided by the manufacture is shown in Table 1.

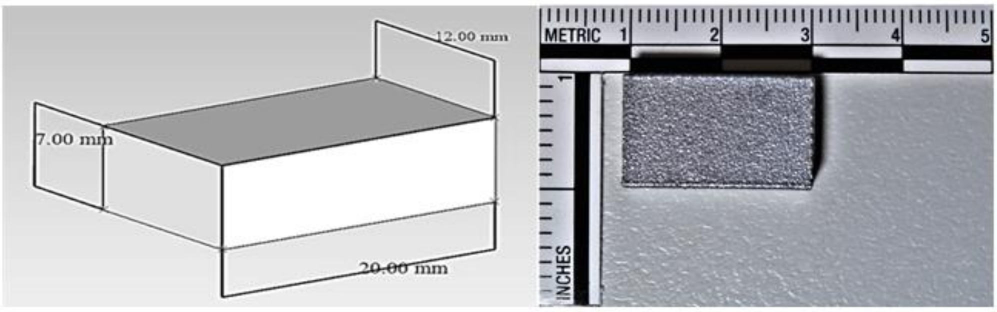

Figure 11. CAD file design and as-built object of all fifteen samples.

Table 3. Chemical composition of the AlSi10Mg alloy starting powder as specified from the manufactures of the two different 3D printers (wt. %)

	AL	Si	Mg	Cu	Fe	Mn	Zn	Ti	Ni	Pb	SN
SLM280 HL	Bal	9 - 11	0.2 - 0.45	0.05	0.55	0.45	0.10	0.15	0.05	0.05	0.05
ProX320	Bal	9 - 11	0.2 - 0.45	0.10	0.55	0.35	0.10	0.15	0.05	0.05	0.05

2.1 Analysis

2.1.1 Optical microscopy

The surface homogeneity of the as-built and finished samples was compared for surface structures by optical microscopy, using a Nikon SMZ18 Stereomicroscope fitted with an x1 objective, x10 eyepieces, and a 60mm working distance. Initial surface observations of the ten as-built samples were made with 10µm and 20µm magnification. The final analysis for the layer width was taken from fifteen random measurements on all ten SLM and DMLS samples at 50µm magnification. Analysis of any differences between the fifteen measurements taken on all samples was conducted in R Studio. Surface observations of the four finished samples were made with 0.75µm magnification.

2.1.2 Scanning electron microscopy

The characterisation of the interior microstructures in the as-built samples was accomplished by sectioning all the samples along the XY and Z axis's, followed by polishing with FlexOvit 1200 grit and etched using a Nital solution of 5% Nitric Acid in 100% ethanol.

The prepared samples were examined by scanning electron microscopy, using a JEOL JSM-6000 with EDS for chemical composition analysis.

2.1.3 X-ray diffraction

Peak analysis was performed on both the as-built samples and raw AlSi10Mg powder. The as-built samples were prepared by removing approximately 20g of powder from the DMLS and SLM samples, and the raw AlSi10Mg powder was supplied by the manufacturer. X-ray diffraction analysis was accomplished using a GBC EMMA X-ray diffractometer with settings of 35KV/28mA, with a scanning speed of 2°/minute with reflections in the 2Θ range of 40 - 80°.

3. Results and Discussion

The analysis of 3D printed objects was undertaken using current forensic methods such as optical microscopy, SEM, and XRD. The potential of these forensic methods in the comparison of 3D objects to identify the source printer is currently unknown.

3.1 Optical microscopy

The initial optical microscopy observations of the surface homogeneity of the as-built SLM and DMLS within samples showed surface to be the same between each sample. The comparison of the surface homogeneity between the SLM and DLMS process indicates that the DMLS samples have a slightly less rough surface than the SLM samples, along with pore formation in both SLM and DMLS samples as seen in figure 3.

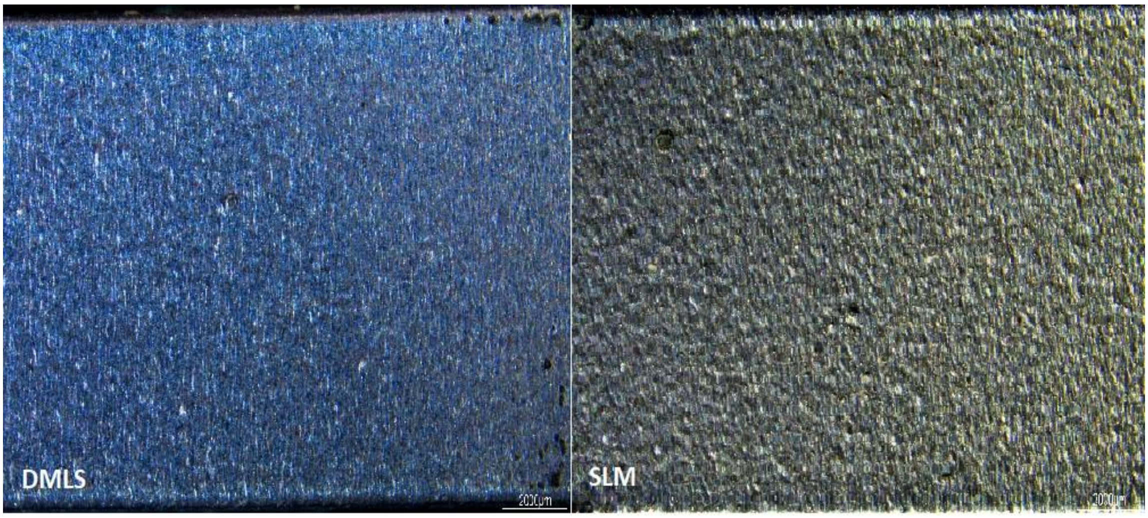

Figure 2. Surface roughness of DMLS and SLM samples at 2000μm.

The finished DMLS and SLM samples were further analysed by optical microscopy for engineering microstructures and pore formation. both the hand and machine polishing are shown to have no distinguishing features other than minor etching from the polishing process (Figure 4).

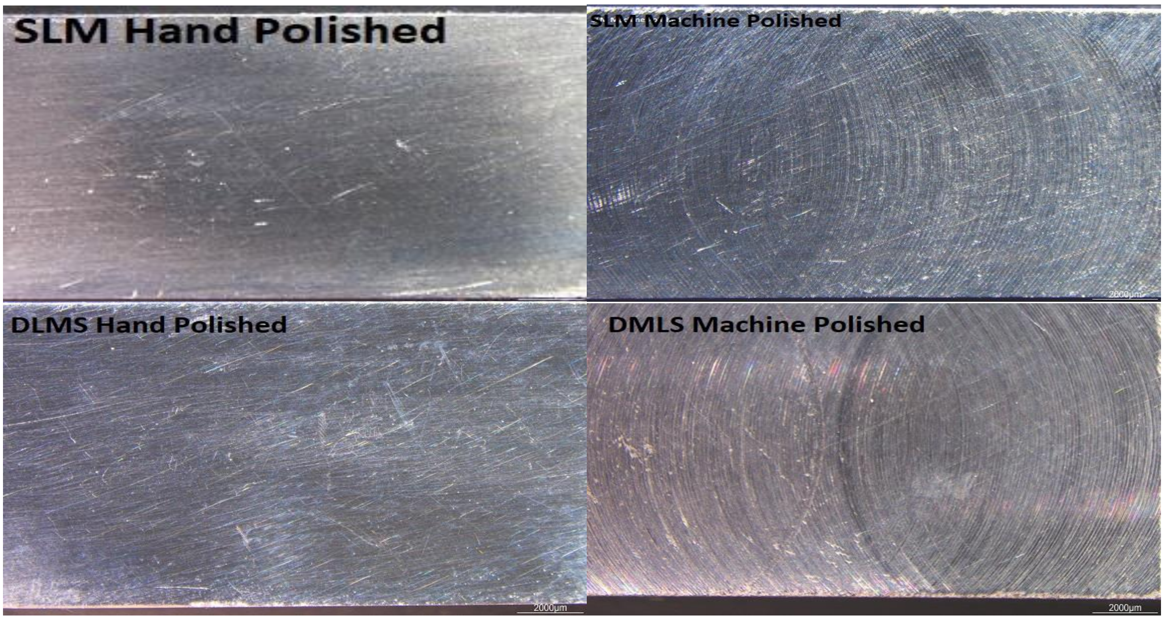

Figure 3. Optical microscopy showing the surface of SLM and DMLS hand and machine polished samples.

The fifteen random measurements of the manufacturing layering as-built samples (not polished) were plotted to determine any variance between the SLM and DMLS processes.

Figure 5 shows that both the SLM and DMLS as-built aluminium objects have similar mean variances. The DMLS process does have three outliers while the SLM process has one outlier, possibly due to measurement error.

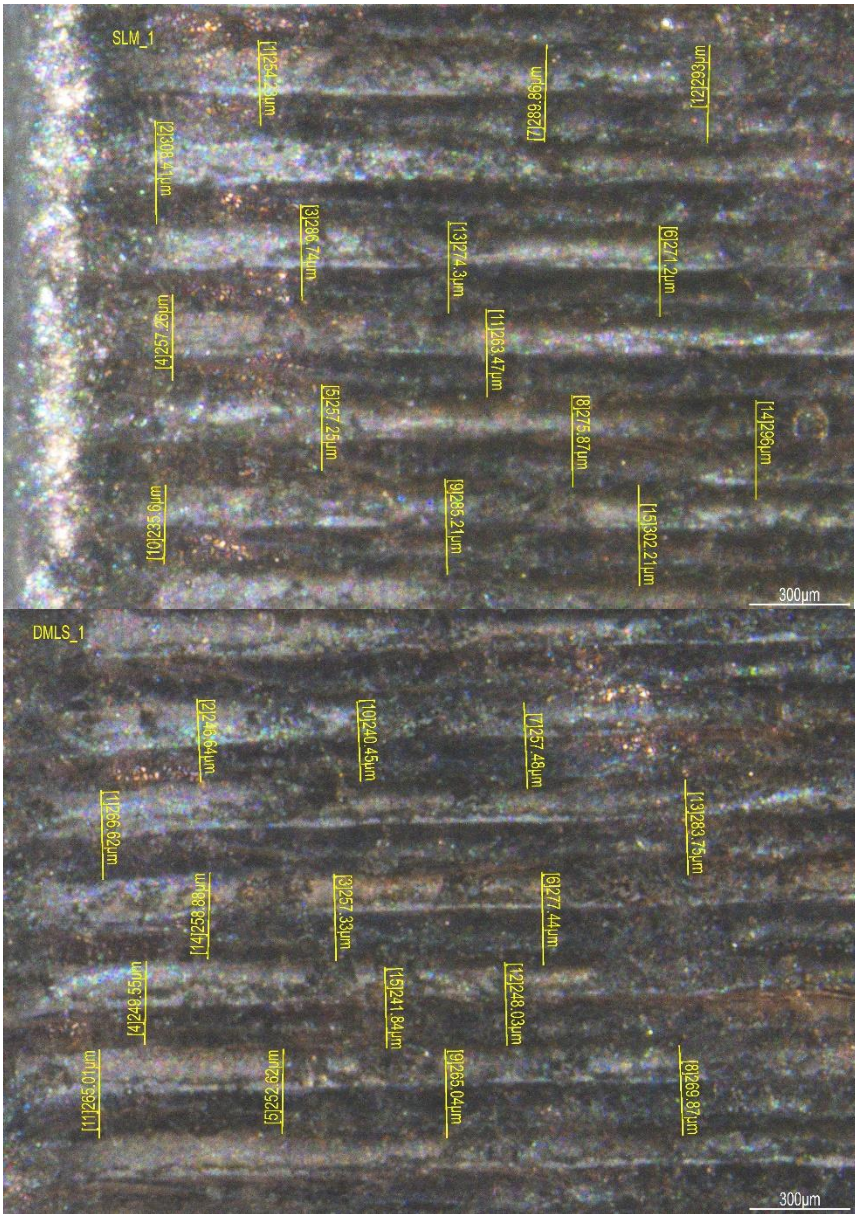

Figure 4. *Layer m*easurements *by* optical microscopy analysis on SLM and DMLS samples.

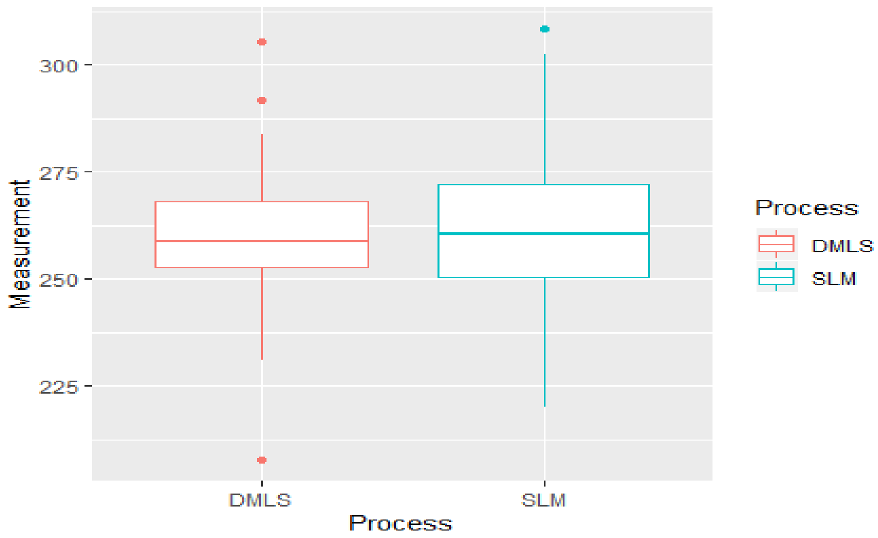

Figure 5. Box plot showing the mean-variance between the SLM and DMLS processes.

A two-way ANOVA was performed on the surface layer features to determine if there is a statistically significant difference in the homogeneity between the SLM and DMLS layering process. Table 2 shows a p-value (0.53) which is greater than 0.05, therefore equal variance can be assumed, and there is no statistical difference between the surface layer features of the SLM and DMLS processes.

The surface layer features were further analysed to determine if there is a statistical difference in the as-built samples generated using the same process. From table 2, the p-value (0.05) shows that there is no statistical difference in the surface homogeneity of aluminium objects printed by the same process.

Table 4. Two-ANOVA of between and within SLM and DMLS samples

	Df	Sum Sq	Mean Sq	F value	Pr(>F)
Process	1	99	98.9	0.397	0.5297
Sample No	4	2413	603.3	2.421	0.0511
Residuals	144	35884	249.2		

The optical microscopy comparison of as-built aluminium objects manufactured with the SLM and DMLS 3D printing processes showed that the surface homogeneity of the samples generated by the same process and between the two processes to be similar with the two way ANOVA showing no difference in the surface features and layering process. It can, therefore, be concluded that the optical microscopy method used in the forensic analysis could not distinguish between the objects produced by SLM or DMLS 3D printing process.

3.2 Scanning electron microscopy

The surface of the DMLS and SLM as-built samples were etched to observe their microstructures. Figure 6 shows the SEM images of the surface features viewed in the XY orientation. Both the SLM and DMLS samples show possible cellular dendrite formation in figure 6. The comparison of the surface microstructures shows random circular or irregularly shaped pores in both sets of samples. The DMLS samples showed slightly larger pore formation Figure 6.

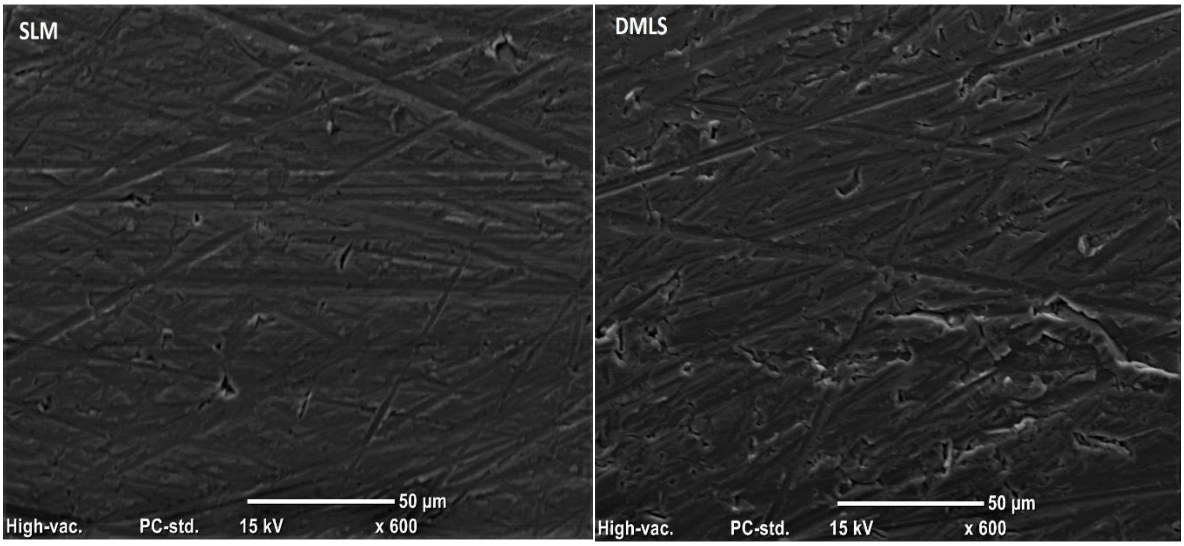

Figure 6. SEM of SLM and DMLS aluminium microstructures.

Scanning electron microscopy can be a valuable forensic method for the analysis and comparison of materials, through the examination of microstructures present on the found object. After etching the SLM and DMLS as-built samples, the surface microstructures were seen to be similar in structure pattern. There was no discernible pattern seen in the pore formation in both sets of samples. The crisscrossing pattern seen in figure 6 possibly indicates the presence of surface fracture channelling as noted by Asgari [57]. From the results observed, it can be concluded that the SEM method of analysis can not discern any differences between as-built SLM and DMLS 3D printed objects.

3.3 X-ray diffraction

X-ray diffraction analysis was performed on the SLM and DMLS as-built samples and raw powder materials. Analysis of the powder peak profile from the four powder samples is shown in figure 8.

The XRD comparison of the SLM and DMLS as-built and raw powder identified the major aluminium (Al) with Silicon (Si) constituents only, as seen in figure 8. The intensity of the Si peak is comparably lower than the AL peaks in all the samples due to the relative weight percentage. The Al peak intensity between the DMLS as-built and raw powder can be seen as relatively similar (92.6 – 93.2%), where the peak intensity between the SLM as-built and raw powder shows a slight variation (98.5 – 89.9%) figure 8. XRD characterisation of crystalline structures using the Rietveld refinement technique can be determined as being cubic for all four powder samples.

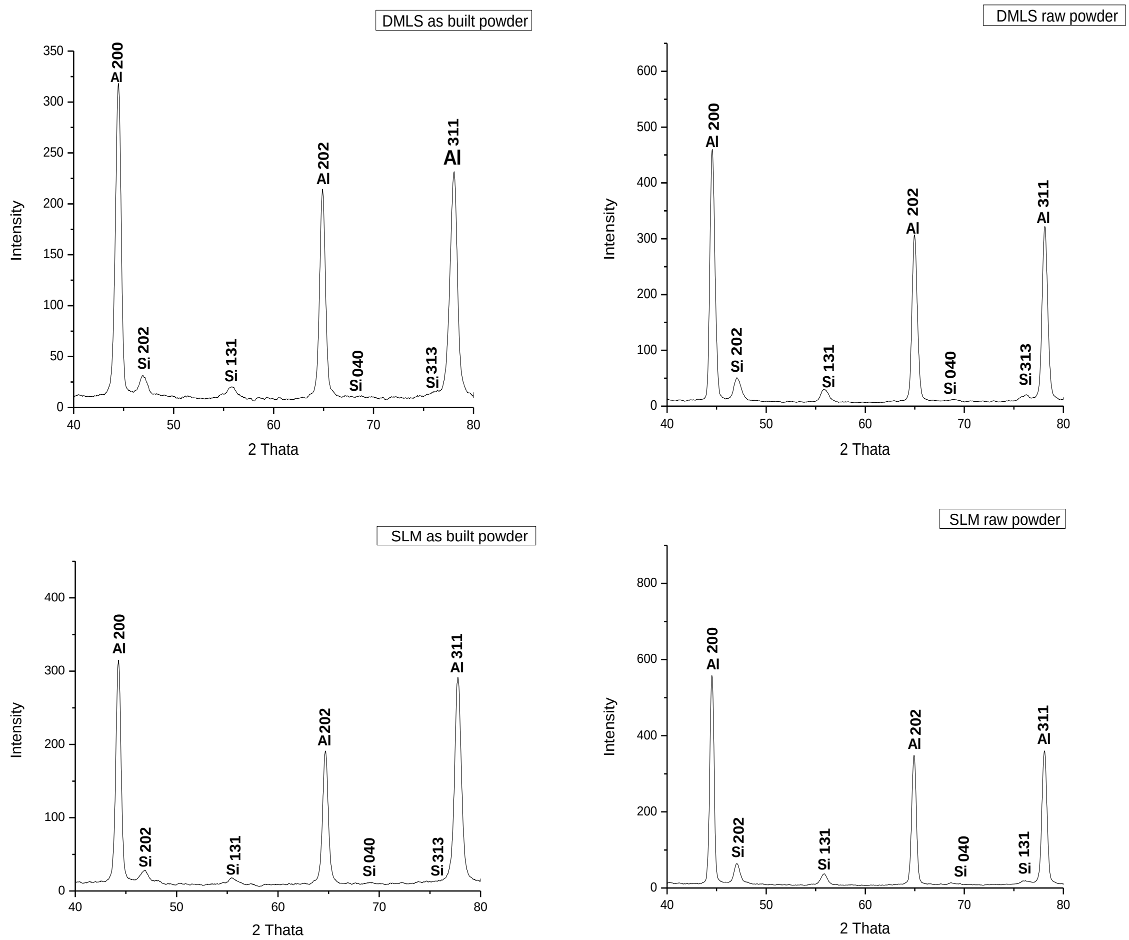

Figure 7. XRD phase pattern, showing miller indices of SLM and DMLS as-built and raw powder.

The peak profile observed by XRD analysis of both the raw and as-built powder showed no difference between the AlSi10Mg powder used by the two manufacturing companies. The phase analysis of the raw starting material shows aluminium and silicon in both samples with the same indices values; however, the DMLS raw powder did have a higher peak intensity that the SLM raw powder. From the XRD results, it can be concluded that XRD analysis is not suitable to differentiate between different AlSi10Mg raw starting material.

4. Conclusion

The experimental techniques used in this research, to evaluate the potential to identify differences in Aluminium alloy object manufactured by the SLM and DMLS 3D printing did not demonstrate statistical differences between them.

Although the current research has shown no differences between the SLM and DMLS printing processes, it is recommended that further research into the comparison of the physical and chemical characterisation of other metal 3D printing processes and materials for the possible identification of the source printer. Further research is needed to evaluate both the SLM and DMLS printing processes for the development of potential new forensic methods for the characterisation of SLM and DMLS printed objects.

5. References

1. Campbell T, Williams C, Ivanova O, Garrett B. Could 3D printing change the world. Technologies, Potential, and Implications of Additive Manufacturing, Atlantic Council, Washington, DC. 2011.

2. Day PJ, Speers SJ. The assessment of 3D printer technology for forensic comparative analysis. Australian Journal of Forensic Sciences. 2019:1-11.

3. Understanding Design & Process of DMLS 3D Metal Printing [internet] 2018 [cited 2019 Dec 11]. Available from: https://grabcad.com/tutorials/how-to-get-the-most-out-of-3d-metal-printing.

4. Duda T, Raghavan LV. 3D metal printing technology. IFAC-PapersOnLine. 2016;49(29):103-10.

5. Macedo BB. Metal based additive manufacturing: Characterization of geometric distortion of powder bed fusion parts after heat treatment. 2019.

6. ISO. ASTM52900-15, Standard Terminology for Additive Manufacturing – General Principles – Terminology. West Conshohocken, PA,: ASTM International; 2015.

7. Bhavar V, Kattire P, Patil V, Khot S, Gujar K, Singh R. A review on powder bed fusion technology of metal additive manufacturing. Additive Manufacturing Handbook: CRC Press; 2017. p. 251-3.

8. Kruth JP, Mercelis P, Van Vaerenbergh J, Froyen L, Rombouts M. Binding mechanisms in selective laser sintering and selective laser melting. Rapid prototyping journal. 2005;11(1):26-36.

9. Trevisan F, Calignano F, Lorusso M, Pakkanen J, Aversa A, Ambrosio E, et al. On the selective laser melting (SLM) of the AlSi10Mg alloy: process, microstructure, and mechanical properties. Materials. 2017;10(1):76.

10. Sames WJ, List FA, Pannala S, Dehoff RR, Babu SS. The metallurgy and processing science of metal additive manufacturing. International Materials Reviews. 2016;61(5):315-60.

11. Ngo TD, Kashani A, Imbalzano G, Nguyen KTQ, Hui D. Additive manufacturing (3D printing): A review of materials, methods, applications and challenges. Composites Part B. 2018;143:172-96.

12. Vock S, Klöden B, Kirchner A, Weißgärber T, Kieback B. Powders for powder bed fusion: a review. Progress in Additive Manufacturing. 2019:1-15.

13. DebRoy T, Wei HL, Zuback JS, Mukherjee T, Elmer JW, Milewski JO, et al. Additive manufacturing of metallic components–process, structure and properties. Progress in Materials Science. 2018;92:112-224.

14. Zadora G., Brożek-Mucha Z. SEM–EDX—a useful tool for forensic examinations. Materials Chemistry and Physics. 2003;81(2):345-8.

15. Rendle David F. X-ray diffraction in forensic science. Rigaku J. 2003;19(2):11-22.

16. Asgari Hamed, Baxter Carter, Hosseinkhani Keyvan, Mohammadi Mohsen. On microstructure and mechanical properties of additively manufactured AlSi10Mg_200C using recycled powder. Materials Science and Engineering: A. 2017;707:148-58.